The impact of the atmosphere on the Eyjafjallajökull 2010 eruption plume

G. N. Petersen,[1] H. Bjornsson,[1] and P. Arason[1]

Received 23 August 2011; revised 2 November 2011; accepted 7 November 2011; published 6 January 2012.

[1] The eruption of Eyjafjallajökull volcano in 2010 lasted 39 days, 14 April–23 May. The eruption had two explosive phases separated by a phase with lava formation and reduced explosive activity. During the explosive phases there were episodes of strong winds that advected ash to the south and southeast leading to widespread disruptions in air traffic. The height of the eruption plume was monitored with a weather radar and with web cameras mounted with a view of the volcano. Three different types of the impact of the ambient atmosphere on the eruption plume are described. First, the weather situation throughout the eruption has been analyzed. The frequency of northerly wind component is found to be unusually high, or 71% in comparison to 49% on average in spring. Secondly, during the effusive phase of the eruption diurnal variation was observed in the plume altitude and there is evidence that suggest that nocturnal inversions may have played a role, limiting the rise of the weak plume. Thirdly, images from a web camera were analyzed and the rise of individual cloud heads associated with explosions at the volcano vent mapped. The velocity profiles obtained largely agree with conceptual models of volcanic plumes.

Citation: Petersen, G. N., H. Bjornsson, and P. Arason (2012), The impact of the atmosphere on the Eyjafjallajökull 2010 eruption plume, *J. Geophys. Res.*, *117*, D00U07, doi:10.1029/2011JD016762.

1. Introduction

[2] A volcanic eruption plume enters into an atmosphere that has a pre-existing structure, in terms of temperature, moisture content, stratification, wind and wind shear. The impact of the ambient atmosphere on the plume influences how high into the atmosphere plume material can be lofted and how far afield it can be distributed. Much depends on the strength of the eruption; the weaker it is the more scope there is for the atmospheric variations, such as wind-shear and stability, to make their mark. However, even for strong eruptions, where the plume extends through the tropopause, the stability of the stratosphere will eventually cap its rise and upper level winds will determine its distribution.

[3] Discussion of atmospheric influence can be separated into the local (near source) and the distal (far field) effects. For the former the interactions between plume dynamics and the atmosphere are important, but the latter depend more strongly on the large scale atmospheric circulation and processes that affect the evolution of the physical and chemical properties within the so-called volcanic cloud.

[4] For the near source, simple models have been used to examine the processes of greatest importance. *Woods* [1988] expanded on previous work, by, e.g., *Morton et al.* [1956], *Wilson* [1976], *Wilson et al.* [1978], *Settle* [1978], *Sparks and Wilson* [1982], *Sparks* [1986] and *Wilson et al.* [1987], and examined the dynamically distinct regions of volcanic plumes but did not treat the background atmosphere in any detail. Using a simplified convection model, *Glaze and Baloga* [1996] examined the buoyant rise of a moist plume and its sensitivity to ambient atmospheric conditions. They found indications that the height reached by the plume is strongly affected by the temperature lapse rate and tropopause height, and that differences in these, such as exist between the tropics and higher latitudes, could have a significant impact on plume height. *Bursik* [2001] examined the influence of the ambient wind strength, as stronger wind will act to increase the entrainment rate of ambient air and lower the altitude at which the plume becomes neutrally buoyant. Furthermore, *Carazzo et al.* [2008] showed that atmospheric stratification can induce variations in entrainment and thus also affect the maximum altitude reached by the plume.

[5] Numerical weather prediction (NWP) models have also been used to study the near source processes. In a systematic sensitivity study, *Graf et al.* [1999] found that ambient wind, static stability as well as ambient temperature and humidity, all affected the maximum altitude reached by the plume. The influence of stability is not surprising, since any departure from ambient neutral stability will act to either increase or decrease the buoyancy force driving the updraft throughout the convective rise of the plume. Further evidence for this was found in a modeling study by *Tupper et al.* [2009] who showed that the modeled plume from a relatively weak volcanic eruption rose 9 km higher under moist tropical ambient conditions than in a dry sub-polar environment. Studies on the influence of volcanic eruptions on climate have also documented differences between eruptions that occur in the

[1]Icelandic Meteorological Office, Reykjavík, Iceland.

tropics and mid- or polar latitudes [*Robock*, 2000; *Oman et al.*, 2005].

[6] The far field dispersal of volcanic plume constituents (e.g. ash and SO_2) will depend on how high the plume reaches and the winds aloft, and thus atmospheric movement on synoptic and larger scale. The range is also determined by various in-cloud processes that occur as the volcanic cloud is advected with the wind, especially processes affecting the aggregation and sedimentation rate of volcanic particles.

[7] The far field distribution has been the subject of intense research, since volcanic ash has in the past disrupted air traffic with considerable economic consequences [*Prata*, 2009; *Prata and Tupper*, 2009]. The far field distribution of the ash cloud may be modeled with dispersion models such as NAME, HYSPLIT and Flexpart [*Leadbetter and Hort*, 2011; *Witham et al.*, 2007; *Draxler and Hess*, 1998; *Stohl et al.*, 1998] that predict the advection of the volcanic cloud using numerical predictions of atmospheric fields (such as wind and precipitation) as input.

[8] Typically, the evolution of the ash cloud will be influenced by differential advection whereby the atmospheric circulation advects one part of the ash cloud faster or even in a different direction than other parts, leading to patterns in the cloud extent that are known to be associated with advection [*Welander*, 1955]. The evolution of the ash cloud will also be influenced by synoptic scale features, such as uplift or subsidence [*Dacre et al.*, 2011]. Such features are generic in maps of tracers advected with the atmospheric circulation. In general, remote sensing of volcanic cloud constituents supports the results of dispersion models, although not always in detail [*Witham et al.*, 2007; *Dacre et al.*, 2011].

[9] Studies of the interaction between the atmosphere and the volcanic plume tend to focus on large eruptions. For medium-sized and small explosive eruptions less has been documented on the impact of the ambient atmosphere, most likely due to lack of observations and long term impact.

[10] The 39 day eruption of Eyjafjallajökull in 2010 represented a unique opportunity to observe the influence of the ambient atmosphere on the evolution of a volcanic plume from a relatively small eruption, but one which had several different phases with different characteristics of atmospheric impact.

[11] This paper describes three examples of the influence of the ambient atmosphere on the volcanic plume. First we describe the impact of the atmospheric circulation during the eruption on the advection of the volcanic ash from Eyjafjallajökull volcano and discuss how typical this kind of weather situation is. Then we present an example of a diurnal variation in the eruption plume altitude during the effusive phase of the eruption where the stability of the atmosphere may have played a large role. In the last example the evolution of individual bursts from the volcano is examined. The purpose of this paper is to present evidence from observations of the impact of the atmosphere on an eruption plume of a medium-size explosive eruption, from the larger scale features controlling the downstream advection and dispersion of volcanic ash to the small scale features of the convective phase of the plume. Another example of the impact of the ambient atmosphere on the Eyjafjallajökull eruption plume is given by *Arason et al.* [2011b] where it is suggested that the ambient atmospheric temperature had significant impact on lightning activity in the plume. The arrival of the ash from Eyjafjallajökull 2010 over the continental Europe is a subject of numerous papers, based on both observations and model simulations [e.g., *Dacre et al.*, 2011; *Devenish et al.*, 2012; *Emeis et al.*, 2011; *Schumann et al.*, 2011], and is outside the scope of this paper.

[12] The structure of this paper is as follows. In section 2 we discuss shortly the data, the observations of the eruption plume, from a weather radar and web cameras, and the ambient atmosphere, from radiosondes as well as atmospheric analysis. In section 3 we give an overview of the weather situation during the eruption. Section 4 presents the diurnal cycle in the plume height during the effusive phase of the eruption and section 5 the rise of individual cloud bursts associated with explosions at the volcano vent. Finally there are some concluding remarks.

2. Data Sets

2.1. Atmospheric Data Sets

[13] Upper air soundings of the atmosphere are made twice a day at the Keflavík International Airport in southwest Iceland and here the observations of wind speed and direction at the 500 hPa level are used to assess the prevailing winds over Iceland during the eruptions. To place the weather situation during the eruption in a climatic context all accessible observed data of wind speed and direction at the 500 hPa level are examined, i.e. 18 years of data, 1993–2010. Furthermore, the global reanalysis of the National Centers for Environmental Prediction/the National Center for Atmospheric Research (NCEP/NCAR) [*Kalnay et al.*, 1996; *Kistler et al.*, 2001] is used to describe the large scale atmospheric flow and anomalies. Finally the operational global numerical analysis of the European Centre for Medium-Range Weather Forecasts (ECMWF) is used as initial and 6-hourly boundary condition for numerical simulations of the ambient atmosphere during the effusive period of the eruption.

2.2. Eruption Plume Altitude Data Sets

[14] The C-band weather radar at Keflavík International Airport was the only operational weather radar in Iceland during the eruption. Since its installation in 1991 the radar has been used for monitoring seven volcanic eruptions in Iceland: Hekla in 1991 [*Larsen et al.*, 1992], Gjálp in 1996, Grímsvötn in 1998, Hekla in 2000 [*Lacasse et al.*, 2004], Grímsvötn in 2004 [*Vogfjörd et al.*, 2005; *Oddson*, 2007], Eyjafjallajökull in 2010 and lastly Grímsvötn in 2011. During the eruption in 2010 radar scans were made every 5 min and the data archived at the Icelandic Meteorological Office. Due to the distance from the radar to the eruption site as well as orographic blockage the radar cannot detect a volcanic plume, or clouds, below 2.9 km in altitude over Eyjafjallajökull. This means that the lowest detectable plume top altitude is about 1.2 km above the 1666 m high volcano. A time series of the estimated plume top altitude has been constructed from the radar data. During the eruption radar estimates of the altitude of the volcanic plume were available 45% of the time. The reasons for non-availability were that (i) the altitude of the volcanic plume was below radar detection limits (27% of the time), (ii) the plume was obscured by precipitating clouds (11%), (iii) the radar scans were missing (7%) and (iv) short range doppler scans

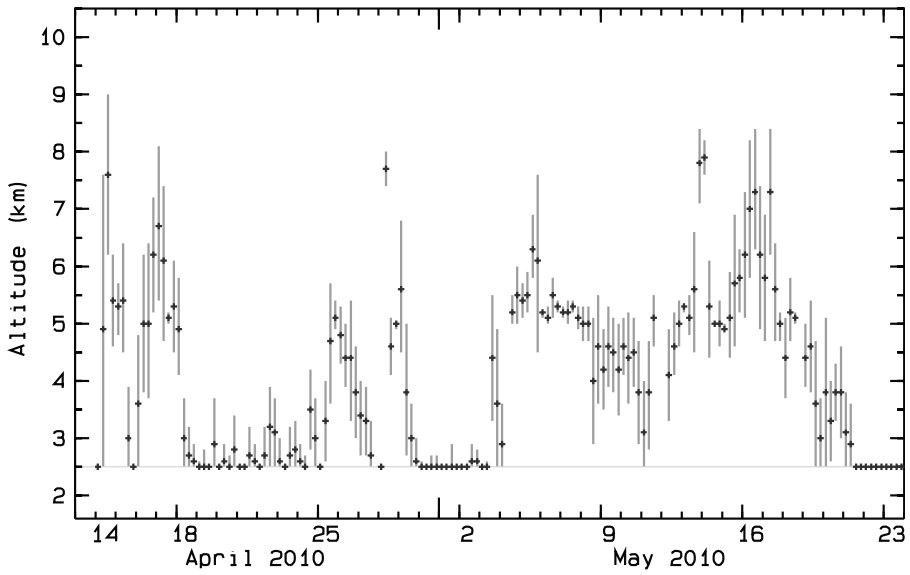

Figure 1. A time series of the 6-hour average altitude (km a.s.l.) of the plume top as observed by the weather radar at Keflavík International Airport. The bars represent one standard deviation. When the volcanic plume was below radar detection limits but other measurements confirmed continued eruption the altitude is assumed to be 2.5 km.

for weather monitoring were made twice per hour following 29 April (10%).

[15] Several web cameras were mounted with a view of the volcano. Their main purpose was to allow the general public to follow the eruption in real time but the cameras were also found to be useful for scientific monitoring. The most useful camera for monitoring the height evolution of the plume was owned by the telecommunication company Míla. The camera was located in the village of Hvolsvöllur, 34 km from the volcano, and had a clear view of the volcano and the sky above up to about 5.2 km a.s.l. The web camera images were saved every five seconds, with vertical resolution at the volcano of about 15 pixels per 100 m. While the duration of the eruption was 39 days the camera only afforded a clear view of the plume for a few of these days. On an hourly basis there was a clear view of the plume-top 17% of the time in addition to instances when the plume penetrated above the frame of the images (5%). Furthermore it has been estimated that due to wind effects the uncertainty in the web camera plume-top altitudes is on the order of 10% [*Arason et al.*, 2011a].

[16] *Arason et al.* [2011a] describe in more detail the radar and the web camera data and their limitation. They conclude that although the web camera plume altitudes are more accurate than the radar-estimates, the availability of the radar estimates is much higher. Therefore, despite inaccuracies in the data weather radars are very useful devices for monitoring volcanic plumes.

3. The Weather Context of the Eruption

[17] Figure 1 shows a time series of 6-hourly average altitude of the volcanic plume as observed by the weather radar at Keflavík International Airport. The eruption had four distinct phases and these can be seen in Figure 1: The first explosive phase (14–18 April), the effusive phase (18 April–3 May), the second explosive phase (3–17 May) and the final phase (18–22 May). During the effusive phase lava was flowing beneath the glacier and melting ice. This resulted in a steam plume, sometimes exceeding 4 km in altitude, while the ash plume itself was much lower. As mentioned earlier the eruption lasted 39 days, being the longest eruption in Iceland since Hekla in 1991. Also, together the two explosive phases exceeded by far the duration of any explosive eruption phase in the last 30 years, see Table 1. This is also the only eruption in Iceland in decades resulting in southerly to easterly ash advection away from Iceland. Consequently the eruption caused widespread disruption to aviation throughout Europe [e.g., *Petersen*, 2010]. Thus, it is of interest to investigate the weather regime of the eruption period and discuss if this was an unusual situation.

[18] Convective activity during spring in Iceland is in general weak. The frequency of rain shower, snow shower and thunderstorm reports from manned weather stations in S-Iceland was low during the eruption, similar as in other springs. Thus, it does not appear that the atmosphere was primed for convection as has been observed in a tropical setting [*Tupper et al.*, 2005].

[19] Figure 2 shows the time series of observed wind direction at 500 hPa at Keflavík airport as well as an interpolated wind speed as a function of altitude. There were strong westerly winds over Iceland during the first two days of the eruption, with wind speed exceeding 50 m s^{-1} at 7–10 km altitude (see Figure 2b). However, from 17 April northerly winds were prevailing (see Figure 2a). In fact, during most of the first explosive phase strong upper level winds advected volcanic ash to the southeast (towards Europe) while during the second explosive phase the volcanic ash was transported in a more southerly direction from Iceland (over the N-Atlantic). There were two periods with transport towards north: during the effusive phase and then again during the final phase of the eruption. In both cases

Table 1. Notable Explosive Eruptions in Iceland 1970–2011, the Starting Date, the Duration, the Duration of the Explosive Phase and the Direction of Ash Dispersal Away From Iceland

Volcano	Date	Duration	Explosive Phase	Direction of Ash Dispersal	References
Hekla	5 May 1970	61 days	~2 hours	North-northwest	*Thorarinsson* [1970], *Thorarinsson and Sigvaldason* [1972]
Hekla	17 August 1980	3 days	~8 hours	North	*Grönvold et al.* [1983]
Hekla	9 April 1981	8 days	Few hours	North	*Grönvold et al.* [1983]
Hekla	17 Jan 1991	53 days	~10 hours	North-northeast	*Larsen et al.* [1992], *Gudmundsson et al.* [1992]
Gjálp	30 Sept 1996	13 days	13 days	North	*Gudmundsson et al.* [1997]
Grímsvötn	18 Dec 1998	10 days	10 days	Varied	*Gudmundsson et al.* [2000]
Hekla	26 Feb 2000	12 days	~12 hours	North and north-northeast	*Lacasse et al.* [2004]
Grímsvötn	1 Nov 2004	6 days	6 days	Northeast	*Sigmundsson and Gudmundsson* [2004], *Vogfjörd et al.* [2005]
Eyjafjallajökull	14 April 2010	39 days	5 and 24 days	Mainly south, southeast and east	
Grímsvötn	21 May 2011	8 days	8 days	Mainly south	

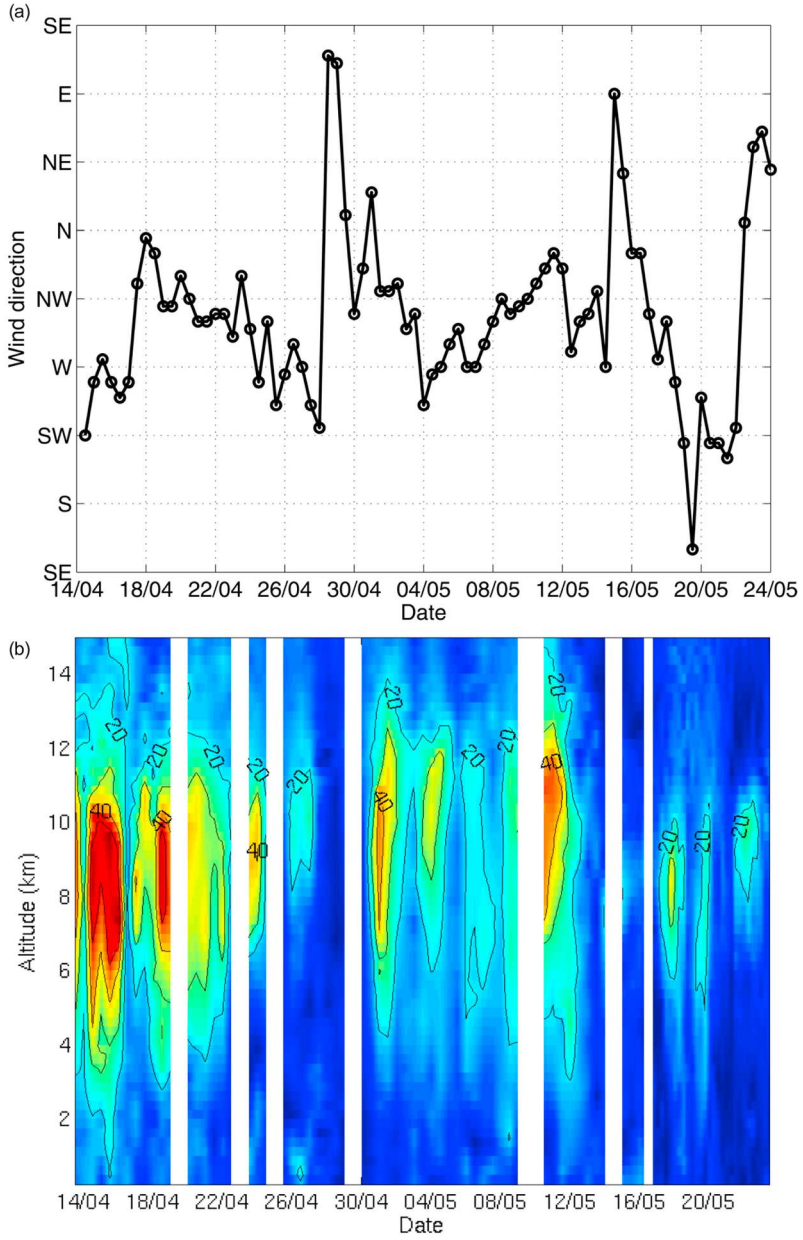

Figure 2. Time series of observed (a) wind direction at 500 hPa and (b) interpolated wind speed (m s^{-1}) as a function of altitude at Keflavík International Airport, 14 April–23 May 2010.

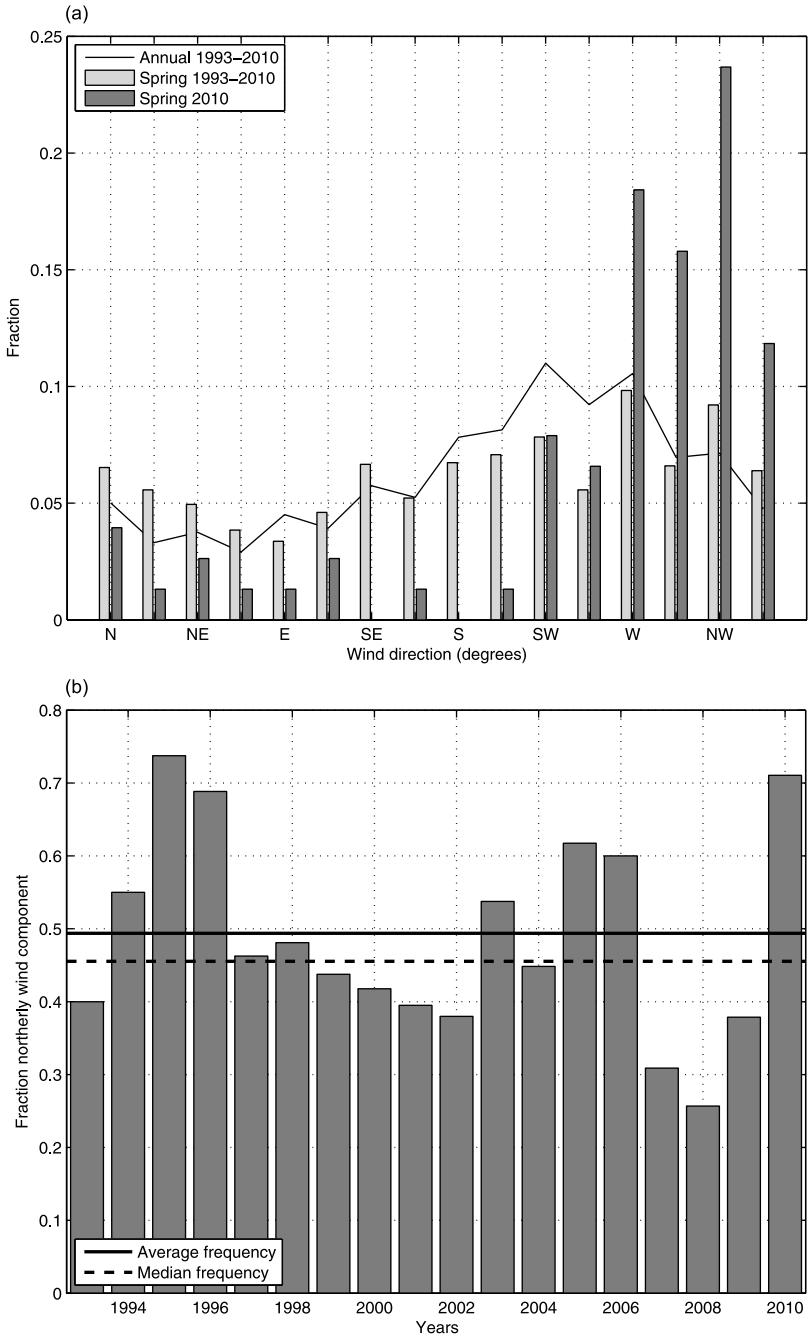

Figure 3. (a) The observed frequency of wind direction at 500 hPa level at Keflavík International Airport. The curve shows the mean annual frequency for 1993–2010 while the bars show the frequency for the spring period (14 April–23 May) of 1993–2010 (light gray) and for only 2010 (dark gray). (b) The observed frequency of northerly wind component in spring for 1993–2010. The average frequency (solid line) and the median frequency (dashed line) are also shown.

ash production was much less than during the two explosive phases.

[20] The prevailing wind direction during the eruption can be put into a climatic context by comparing the frequency of wind directions with a longer term frequency. For this comparison we use the observed frequency of wind directions at 500 hPa level at Keflavík International Airport. The time period is the eruption period 14 April–23 May, for simplicity hereafter termed 'spring', in 2010 compared to the mean spring frequency for the 18 year period 1993–2010 (see Figure 3a). In addition, the annual frequency is also shown in Figure 3a. Figure 3a shows that in general, on an annual basis, southerly to westerly winds are the most common (47% of the time), with a slightly more even distribution of wind directions in spring. Frequency of winds with a northerly component during spring is 49%. In contrast,

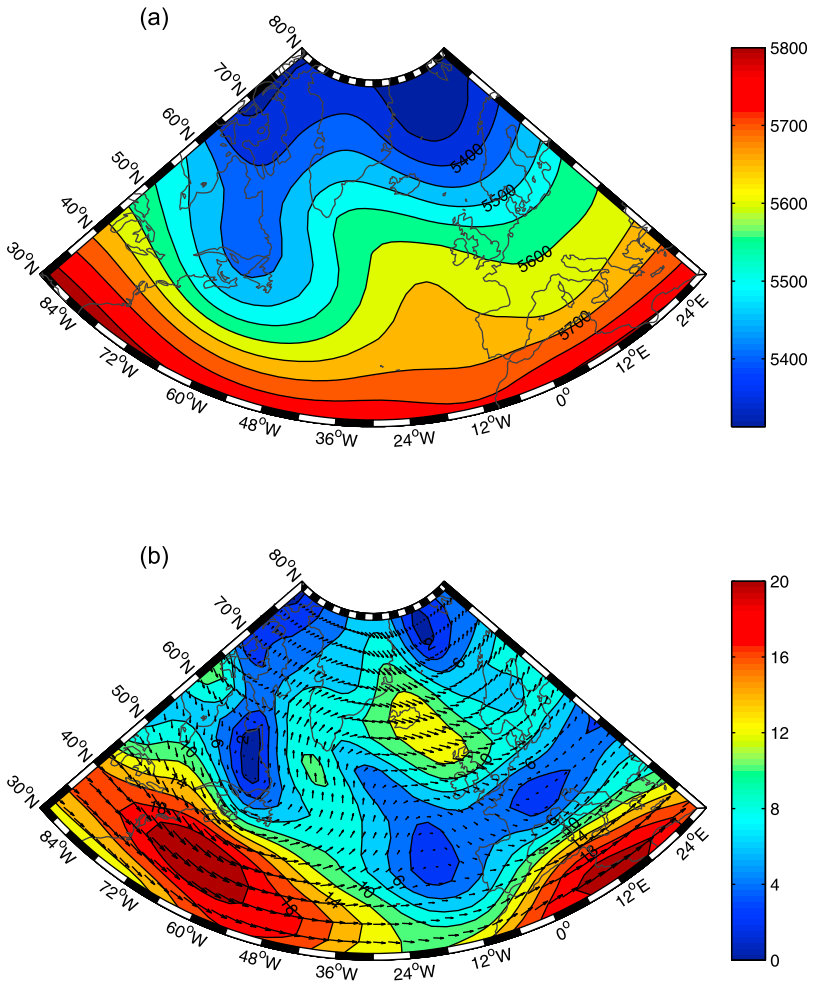

Figure 4. The NCEP reanalysis mean 500 hPa (a) geopotential height (m) and (b) wind speed (m s^{-1}) for the spring period (14 April–23 May) of 2010.

during the spring of 2010 westerly and northwesterly winds dominated. Winds with a northerly component occurred much more frequently, or 71% of the time, and the most common wind direction was northwesterly, occurring 24% of the time.

[21] It should be noted that there is a large annual variability in the wind direction at 500 hPa level in spring. The frequency of a northerly wind component varies from 26% to 74% for the years 1993–2010 (see Figure 3b). However, during 13 out of the 18 springs the frequency of a northerly wind component is within one standard deviation of the average frequency (35–63%), emphasizing the anomalously high frequency of northerly winds during the spring of 2010.

[22] Figure 4 shows the mean 500 hPa geopotential height, wind speed and wind vectors during the eruption in spring 2010 as described by the NCEP/NCAR reanalysis. In the mean there was a trough over the eastern coast of Canada and a high pressure ridge over the North Atlantic. Over and southeast of Iceland the mean wind was northwesterly 12 m s^{-1}. This is a large deviation from the climatological mean as can be seen in Figure 5. The 500 hPa geopotential height anomaly had a tripole pattern over the North Atlantic with a positive anomaly of 130 m over the Irminger Sea, just southwest of Iceland. The 500 hPa meridional wind anomaly over Iceland was 8 m s^{-1}, the largest meridional wind anomaly of the Northern Hemisphere for the period. At the surface high pressure systems over the North Atlantic were the dominant features of the period (not shown). In fact, during the 39 days of eruption high pressure systems dominated the flow pattern during 19 days, 14–21 April and 1–11 May, or almost 50% of the time.

[23] *Leadbetter and Hort* [2011] showed, using the dispersion model NAME, that for an average eruption of Hekla with an initial plume altitude of 12 km it was most likely that the ash would disperse and be transported eastward in the first 24 hours, occupying the airspace over and immediately east of Iceland. Given the prevailing westerly winds the ash would then during the first few days mainly be advected eastward. However, they also noted a small but significant probability of volcanic ash reaching UK domestic airspace already in the first 24 hours. Although these results were obtained assuming an average explosive eruption in Hekla, they can be applied to most medium sized explosive eruptions in Iceland, especially in south Iceland, due to the scale of the atmospheric circulation advecting the ash.

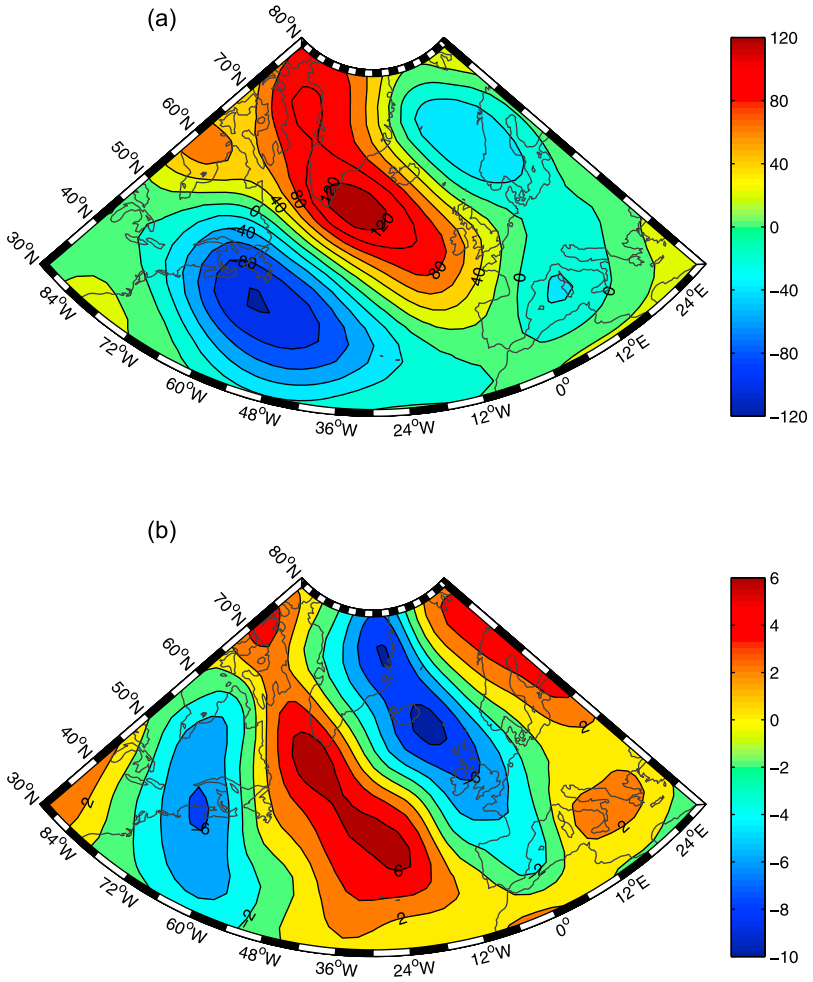

Figure 5. The NCEP reanalysis 500 hPa anomaly of (a) geopotential height (m) and (b) meridional wind component (m s^{-1}) for the spring period (14 April–23 May) of 2010 with respect to the climatology of the spring period 1981–2010.

[24] In summary, the prevailing winds during the eruption of Eyjafjallajökull, that advected the volcanic ash to the south and southeast of Iceland, were unusually persistent and rare. Indeed, for eruptions in recent decades this eruption is the only one where the ash dispersal was to the south and southeast from Iceland (see Table 1).

4. Diurnal Oscillations in the Plume Height

[25] Figure 6a shows a close up of the altitude of the plume as observed by the weather radar 19–24 April 2010, at the start of the effusive phase of the eruption. To show the temporal evolution in more detail during these days, a 3-hour mean altitude is shown instead of a 6-hour mean altitude as in Figure 1. During this period there were no occurrences of precipitating clouds obscuring the plume, but the plume was often below radar detection limits [*Arason et al.*, 2011a]. In fact, the volcanic plume was usually below detection level early in the morning but was observed by the radar in the afternoon. Plotting the data as a function of the time of day shows this more clearly (see Figure 6b): while there were few radar observations of the plume above radar detection limits during the early hours, from midnight to 7 UTC (being equal to Icelandic standard time), the plume altitude increased in the afternoon, peaking at 18–19 UTC with a mean altitude of 3.1 km. This diurnal variation was also observed in the web camera plume altitude estimates.

[26] An inspection of the atmospheric soundings at Keflavík airport during this period reveals weak nocturnal inversions at the top of the atmospheric boundary layer (∼2–4 km altitude) most nights. Figure 7 shows temperature profiles at 00 UTC for four days during the effusive phase. All the profiles show shallow inversions in the height interval 1–2.5 km altitude. The airport is at the southwest coast and 155 km from Eyjafjallajökull; one would expect such nocturnal inversions to be stronger further inland.

[27] To investigate if these nocturnal layers also formed in the region of Eyjafjallajökull a high resolution numerical simulation was run without taking into account the occurrence of the eruption. The numerical weather prediction model Weather Research and Forecasting Model (WRF), Advanced Research version (ARW) V3.2.1 [*Skamrock et al.*, 2005], was used. The model configurations included three domains with horizontal resolution of 9 km, 3 km and 1 km,

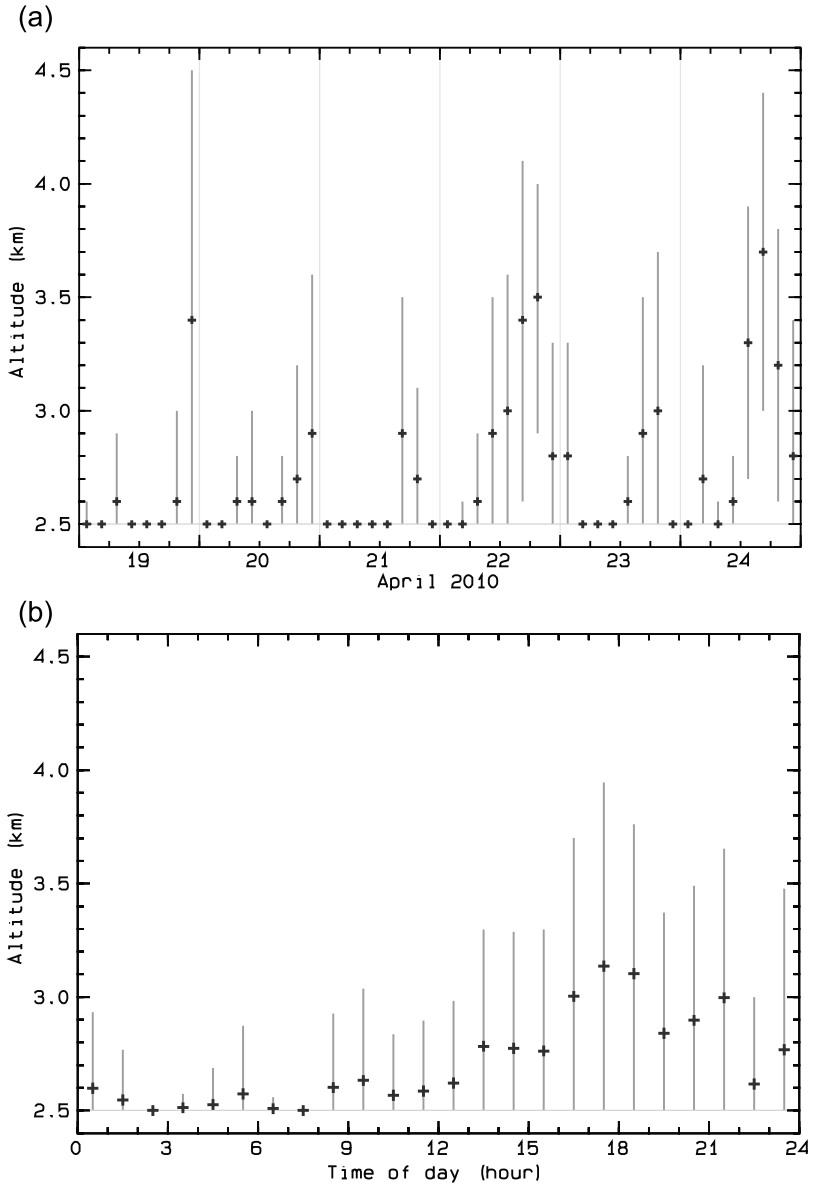

Figure 6. (a) The 3-hour mean plume altitude (km a.s.l.) as observed by the weather radar at Keflavík airport 19–24 April 2010. The bars show one standard deviation. (b) Plume altitude (km) as a function of the time of day for the same period. The crosses indicate the mean and the bars one standard deviation. When the volcanic plume was below radar detection limits but other measurements confirmed continued eruption the altitude is assumed to be 2.5 km.

centered on Eyjafjallajökull. The following physics schemes were applied: The Morrison double-moment microphysics scheme, the Eta similarity surface layer scheme, Noah land surface model, Mellor-Jamada-Janjic planetary boundary layer scheme and the Grell-Devenyi cumulus parametrization scheme. The initial and 6-hourly boundary conditions were retrieved from ECMWF operational analysis and the simulation run for 24 hours. Simulations were run for the whole period 19–24 April 2010. However, not all simulations resulted in a nocturnal boundary layer, most likely due to lack of detail in the initial conditions. Here we show the simulations for 23 April, which includes the most pronounced simulated inversion.

[28] Figure 8 shows the temperature evolution over the volcano on 23 April. The results of the 1 km horizontal resolution simulation show a nocturnal inversion in the vicinity of the volcano that weakens and dissipates during the morning. At 03 UTC there is a weak capping inversion at 2.2–2.6 km altitude. During the morning and early afternoon the air at the lowest levels warms up while the air above the inversion cools due to the expansion of the air column. This results in weakening, and in the end, removal of the inversion.

[29] Capping inversions, such as observed at Keflavík airport and simulated in vicinity of the volcano, can impact the altitude reached by a volcanic plume if they exist close to

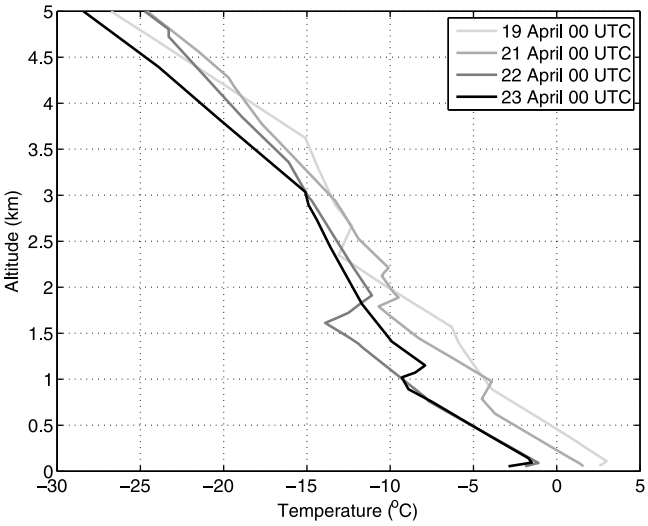

Figure 7. Observed temperature profiles (°C) over Keflavík International Airport 19, 21, 22 and 23 April 2010 at 00 UTC.

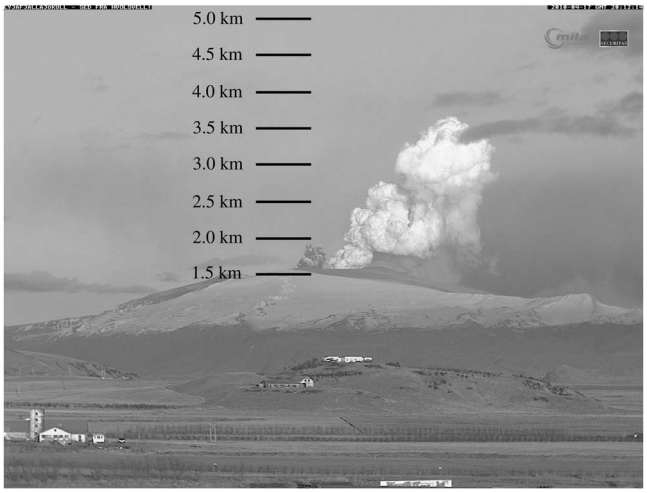

Figure 9. An example of an image from the camera at Hvolsvöllur. The photo is taken at 20:12:14 UTC on 17 April. An approximate height scale valid above the vent (km a.s.l) has been added to the photo.

the neutral buoyancy level of the plume as in this case, thus hampering the growth of the plume in a similar way as the much stronger temperature inversion at the tropopause.

5. Observations of the Plume Rise

[30] Sections 3 and 4 have documented both large scale and local atmospheric influences on the rise and dispersal of the volcanic plume. In this section observations of the plume rise will be presented and discussed in the context of buoyancy and entrainment of ambient air.

[31] Figure 9 shows an example image from the web camera at Hvolsvöllur taken on 17 April at 20:12:14 UTC. The top of the image is at about 5.2 km a.s.l or about 3.5 km above the volcano vent, and an approximate height scale valid above the vent has been added to the image. At this time the plume exhibited intermittent bursts, with few minutes between bursts. These were seen as well defined cloud heads rising into the atmosphere above the volcano. In the image, one such cloud head can be seen above the 3.5 km altitude line, and another burst below the 2 km mark has just exited the vent. As these images were sampled every 5 s they allowed for the tracing of the rising cloud heads. This was done for 10 different bursts on 4 different days during the eruption. In each case a horizontal wind correction was applied by shifting the sequential images horizontally to ensure that the cloud head rose vertically. This was continued for all images until no updraft was detected, the cloud head was obscured by other clouds or it rose out of the image frame. Figure 10 shows the result for a burst that started on 17 April at about 20:08:30 UTC and could be traced until obscured by clouds at about 20:13:30 UTC. An edge detection algorithm was applied on the resulting image and a curve marking the height of the cloud as a function of time was obtained.

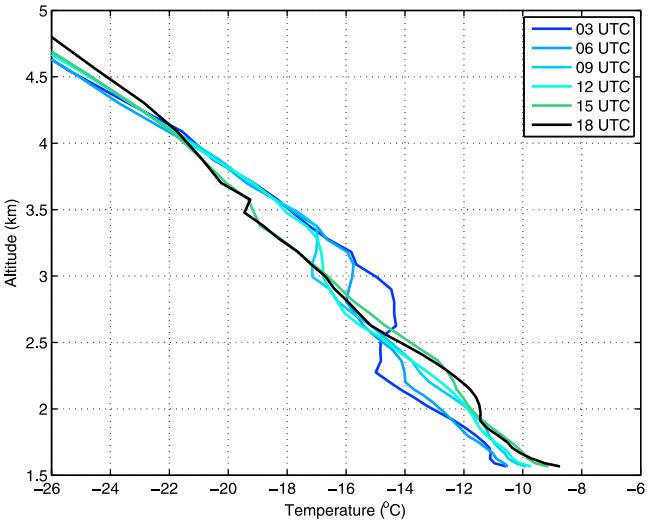

Figure 8. Simulated temperature profiles (°C) over Eyjafjallajökull, initial time 23 April 2010 00 UTC. The curves show the profile from 3 UTC to 18 UTC every 3 hours.

[32] Figure 11 shows the results for the 10 different plume bursts. From 20:03 UTC to about 20:19 UTC on 17 April there were two bursts that rose by 3.5 km in less than 200 s, and one burst that rose 2.5 km in about 300 s. On 20 April two bursts (starting at 06:49:45 UTC and 08:01:16 UTC) were traced for 225 s rising by 1.5 km and 1.8 km, respectively. A day later, the plume bursts were much weaker and two bursts rose by about 0.5 km in approximately 100 s. Following the re-intensification of the eruption in May, a plume burst starting at 13:34:25 UTC on 10 May was tracked for about 225 s rising by about 2.4 km. Later during the same day a burst starting at 15:14:24 UTC was tracked for about 140 s as it rose by about 1.5 km. Finally, on 15 May a burst starting at 17:04:50 UTC was tracked rising by 3.1 km in about 200 s.

[33] The three profiles with the strongest vertical motions (17 April, starting at 20:03:04 and 20:12:09, and on 15 May starting at 17:04:50) rise by 3 km or more in less than 200 second, implying an average speed of 15 m s^{-1} or more. The two lowest profiles (21 April starting 13:02:38 and

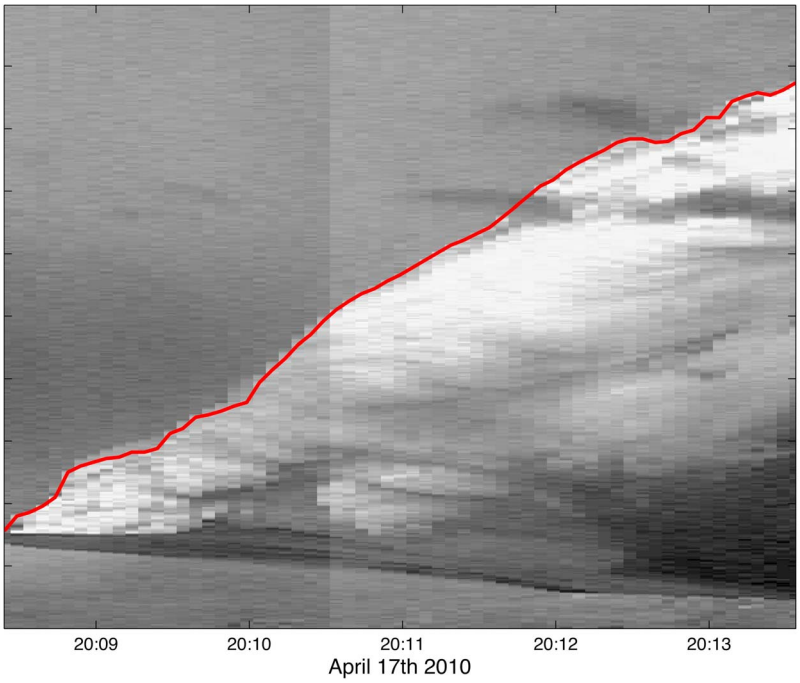

Figure 10. A time slice showing the vertical rise of a cloud head due to a burst from the eruption starting at about 20:08:30 UTC on 17 April and rising into background clouds at about 20:13:30 UTC. The red line shows the result of an edge detection algorithm that traces the edge of the rising cloud.

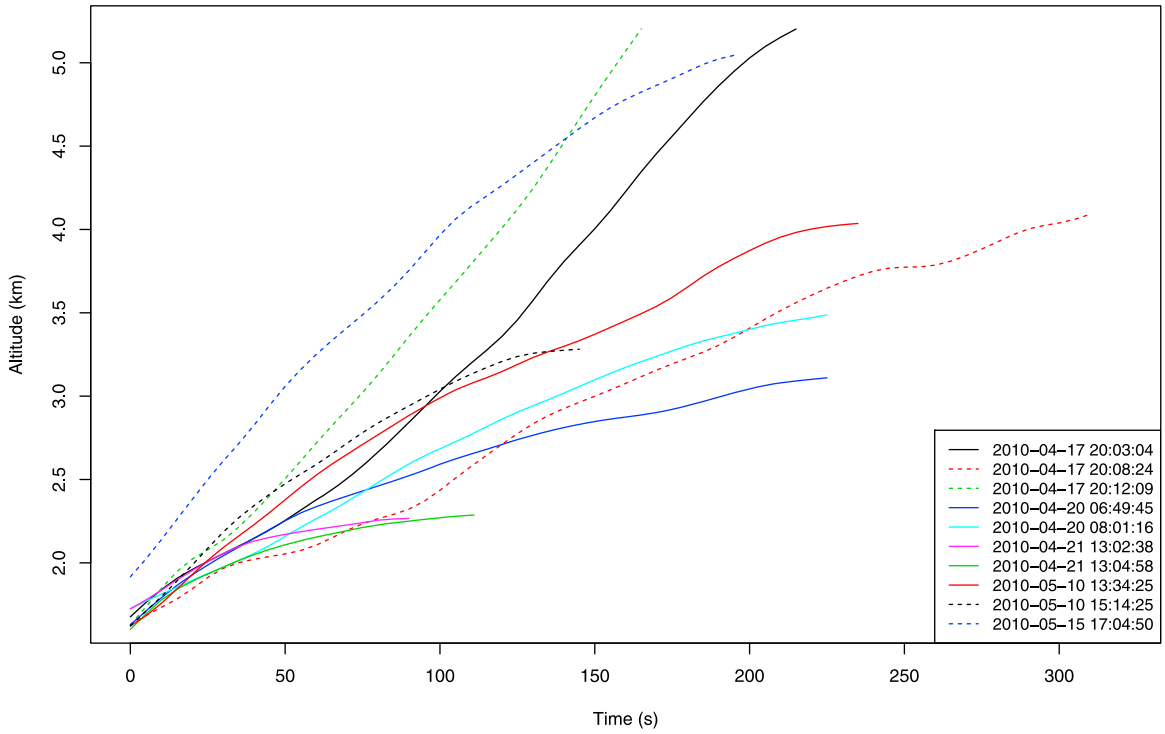

Figure 11. Profiles of cloud head height for 10 different plume bursts. The horizontal axis shows the duration of the cloud rise (s). The legend shows the date and time of initiation of the plume bursts.

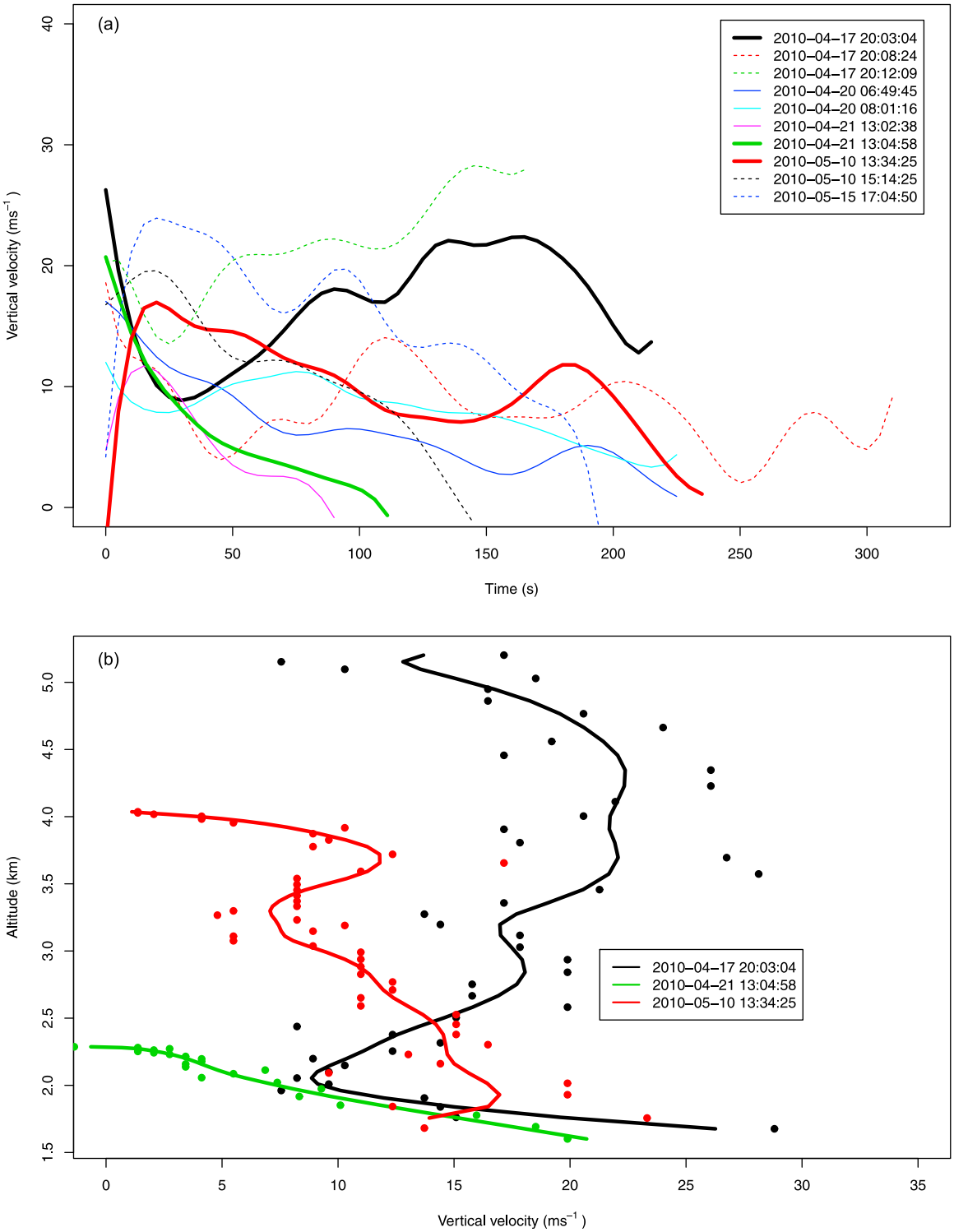

Figure 12. (a) Profiles of the vertical velocity for the 10 different plume bursts calculated using second order finite differencing. The horizontal axis shows the duration of the cloud rise (s). Three cases are shown in boldface; (b) the velocity in these cases as a function of altitude. For visualization, the lines show results where a Gaussian smoothing filter has been applied to the results of the differentiation, but the points in Figure 12b show the unfiltered results.

13:04:58) only rise slightly above 500 m in about 100 s, implying an average speed of 5 m s^{-1}. In between these are profiles that rise by 1.5–2.5 km in about 200 s (i.e. 17 April starting at 20:08:24, 20 April starting at 08:01:16 and 10 May starting at 13:34:25), implying speeds ranging from 7.5–12.5 m s^{-1}. It is interesting to note that two of the fastest rising profiles start about 9 min apart on 17 April and both rise to about 5 km altitude, but in between those is a profile that rises at an intermediate velocity of about 8 m s^{-1} and only rises to 4 km. Clearly these differences cannot be associated with ambient atmospheric influences, but are rather associated with variations in the strength of explosive activity at the vent.

[34] Differentiating the height profiles in Figure 11 yields profiles of velocity. Figure 12a shows the results of applying a second-order finite differencing on all the profiles while Figure 12b shows the velocity as a function of height for a strong, weak and intermediate profile. The lines in Figure 12 show a Gaussian filtering of the results of the differentiation, while in Figure 12b for visualization purposes the unfiltered data points are shown for only three cases.

[35] The conceptual model of a volcanic plume [*Sparks*, 1986] is one where a high velocity mixture of gas and solid particles is injected into the atmosphere at the vent. The mixture is negatively buoyant and initially rises on account of its momentum at the vent. This phase, the gas thrust phase, is limited in extent by the velocity at the vent, but as the plume rises ambient air will be entrained and mixed in. The ambient air warms up, expands and thereby lowers the density of the rising plume. As this process continues the plume eventually becomes positively buoyant and will rise convectively. During the convective phase the maximum height of the plume depends to a large extent on its heat content [*Glaze and Baloga*, 1996], but also on factors such as the rate of entrainment, mass of volcanic ash lofted into the atmosphere by the updraft and mass fallout, as well as ambient moisture and stability [*Mastin*, 2007]. Calculations with simple models [*Woods*, 1988; *Mastin*, 2007] indicate that the plume may accelerate vertically during the early part of the convection phase, followed by a deceleration as it approaches its level of neutral buoyancy. In Figure 12b, two of the profiles show acceleration, but the example from the weak plume shows no such evidence. For the strong plume there is also a suggestion of deceleration at the lowest elevation, indicative of a gas thrust phase. However, it is doubtful whether a 5 second time resolution is sufficient to resolve this phase. Despite this, these results tend to agree with the conceptual model, especially regarding the convection phase where ambient air is entrained as the plume rises to an equilibrium altitude.

6. Concluding Remarks

[36] Although the eruption of Eyjafjallajökull was a medium-size eruption with the volcanic plume rarely rising above 7 km it was unusual in its duration and amount of ash dispersed to the south and southeast of Iceland. During the two explosive phases of the eruption there were episodes of strong winds advecting ash to the south and southeast away from Iceland and one such episode caused widespread disruptions to air traffic.

[37] In the decades leading up to the Eyjafjallajökull eruption there have not been any cases of widespread ash dispersal to the south and southeast of Iceland. However, during the May 2011 eruption of Grímsvötn, some ash was again dispersed in this direction.

[38] As discussed in section 3 the situation in spring 2010 was indeed rather unusual, with a 71% frequency of a northerly wind component compared to 49% on average during the last 18 years, frequent northwesterly winds and a large deviation from the climatological mean circulation. Although the calculated risk of speedy ash dispersal towards UK is low [*Leadbetter and Hort*, 2011] it is obvious, due to e.g. consequences and complications for the air traffic over Western Europe and the North Atlantic, that the likelihood of northerly winds over Iceland during an explosive eruption has to be taken seriously.

[39] The long duration of the eruption gave an opportunity to observe some interesting features of the impact of the atmosphere on the eruption plume, recorded by a weather radar and web cameras. While the radar is a fixed operational instrument for weather monitoring the web cameras were set up to allow the general public to follow the eruption in real time, but proved also quite useful for scientific monitoring. The plume altitude estimates from the most useful web camera were much more accurate than the radar estimates but the availability of data much lower, as there was no detection during darkness or when visibility was low [*Arason et al.*, 2011a]. For future eruptions, in order to retrieve as much information as possible, a few sets containing both a visual and a multispectral camera located strategically around a volcano would be very useful. Similarly, mobile radars located with a clear view of an eruption site would give more detailed information than the radar at Keflavík International Airport. In fact one such mobile radar was operating in Iceland during the eruption of Grímsvötn in 2011. However, as any mobile instruments need to be placed in the field they may not be operating at the start of an eruption. Therefore fixed operational instruments although obtaining lower vertical resolution data, are vital parts of an monitoring system.

[40] During the effusive phase of the eruption the plume height exhibited a diurnal oscillation. Atmospheric soundings from Keflavík and the results of experiments with the WRF model show that a nighttime capping inversion was present at 2.2–2.6 km altitude. The most likely explanation for the diurnal oscillation is that a capping inversion inhibited the rise of the plume, but as the inversion dissipated the plume rose to a higher altitude. Further modeling will consider adding the eruption both as a thermal source and as a source of ash into high resolution simulations with the WRF model and examine in more detail how the inversions affected the plume during this phase of the eruption. The lack of upper-air observations close to the volcano emphasize the need for a mobile radiosonde station. Such observations of the ambient atmosphere are important to understand better how the atmosphere impacts the volcanic plume. Furthermore, increased frequency of soundings at the fixed sounding positions would be advantageous during eruptions.

[41] Vertical velocities of the plume range from 15–20 m s^{-1} on the average, with speed estimates in some instances reaching up to 30 m s^{-1} when the eruption was at

its strongest, to less than 5 m s^{-1} during the effusive phase. The profiles of velocity show signs of the buoyancy driven convective phase of the plume rise, in agreement with idealized models of plume dynamics. Currently, the methodology for tracing the bursts is being improved with the intent of applying it to other periods during the eruption, and also on images recorded with video cameras. An improved methodology that allows us to trace horizontal motions as well as vertical will yield information on the influence of the cross wind on the rise of the plume. This will be examined in a further study.

[42] The eruption of Eyjafjallajökull volcano in 2010 emphasized the importance of understanding the evolution of the plume itself and the need for good information on the size distribution and amount of volcanic ash injected into the atmosphere as well as the injection altitude. Large scale dispersion models rely on this information for their forecasts. Much development is needed in both measurement strategies and high resolution plume simulations in order to improve the near field information. Hopefully the data from Eyjafjallajökull 2010 eruption will help expedite this process.

[43] **Acknowledgments.** Guðrún Larsen assisted in collecting information on explosive eruptions in Iceland during the last decades. Míla ehf. kindly provided the web camera photographs. Three reviewers are thanked for their kind and constructive reviews.

References

Arason, P., G. N. Petersen, and H. Bjornsson (2011a), Observations of the altitude of the volcanic plume during the eruption of Eyjafjallajökull, April–May 2010, *Earth Syst. Sci. Data*, *3*, 9–17, doi:10.5194/essd-3-9-2011.

Arason, P., A. J. Bennett, and L. E. Burgin (2011b), Charge mechanism of volcanic lightning revealed during the 2010 eruption of Eyjafjallajökull, *J. Geophys. Res.*, *116*, B00C03, doi:10.1029/2011JB008651.

Bursik, M. (2001), Effect of wind on the rise height of volcanic plumes, *Geophys. Res. Lett.*, *28*, 3621–3624, doi:10.1029/2001GL013393.

Carazzo, G., E. Kaminski, and S. Tait (2008), On the rise of turbulent plumes: Quantitative effects of variable entrainment for submarine hydrothermal vents, terrestrial and extra terrestrial explosive volcanism, *J. Geophys. Res.*, *113*, B09201, doi:10.1029/2007JB005458.

Dacre, H. F., et al. (2011), Evaluating the structure and magnitude of the ash plume during the initial phase of the 2010 Eyjafjallajökull eruption using lidar observations and NAME simulations, *J. Geophys. Res.*, *116*, D00U03, doi:10.1029/2011JD015608.

Devenish, B. D., J. J. Thomson, F. Marenco, S. J. Leadbetter, and H. Ricketts (2012), A study of the arrival over the United Kingdom in April 2010 of the Eyjafjallajökull ash cloud using ground-based lidar and numerical simulations, *Atmos. Environ.*, doi:10.1016/j.atmosenv.2011.06.033, in press.

Draxler, R. R., and G. D. Hess (1998), An overview of the HYSPLIT4 modeling system of trajectories, dispersion, and deposition, *Aust. Meteorol. Mag.*, *47*, 295–308.

Emeis, S., et al. (2011), Measurement and simulation of the 16/17 April 2010 Eyjafjallajökull volcanic ash layer dispersion in the northern Alpine region, *Atmos. Chem. Phys.*, *11*, 2689–2701, doi:10.5194/acp-11-2689-2011.

Glaze, L. S., and S. M. Baloga (1996), The sensitivity of buoyant plume heights to ambient atmospheric conditions: Implications for volcanic eruptions, *J. Geophys. Res.*, *101*, 1529–1540, doi:10.1029/95JD03071.

Graf, H.-F., M. Herzog, J. M. Oberhuber, and C. Textor (1999), The effect of environmental conditions on volcanic plume rise, *J. Geophys. Res.*, *104*, 24,309–24,320, doi:10.1029/1999JD900498.

Grönvold, K., G. Larsen, P. Einarsson, S. Thorarinsson, and K. Saemundsson (1983), The Hekla eruption 1980–1981, *Bull. Volcanol.*, *46*, 349–363.

Gudmundsson, A., et al. (1992), The 1991 eruption of Hekla, Iceland, *Bull. Volcanol.*, *54*, 238–246.

Gudmundsson, M. T., F. Sigmundsson, and H. Bjornsson (1997), Ice-volcano interaction of the 1996 Gjalp subglacial eruption, Vatnajokull, Iceland, *Nature*, *389*, 954–957.

Gudmundsson, M. T., G. Larsen, H. Bjornsson, and F. Sigmundsson (2000), Comment: Subglacial eruptions and synthetic aperture radar images, *Eos Trans. AGU*, *81*, 134–135.

Kalnay, E., et al. (1996), The NCEP/NCAR Reanalysis 40-year Project, *Bull. Am. Meteorol. Soc.*, *77*, 437–471.

Kistler, R., et al. (2001), The NCEP-NCAR 50-year reanalysis: Monthly means CD-ROM and documentation, *Bull. Am. Meteorol. Soc.*, *82*, 247–267.

Lacasse, C., S. Karlsdóttir, G. Larsen, H. Soosalu, W. I. Rose, and G. G. J. Ernst (2004), Weather radar observations of the Hekla 2000 eruption cloud, Iceland, *Bull. Volcanol.*, *66*, 457–473.

Larsen, G., E. Vilmundardóttir, and B. Þorkelsson (1992), Heklugosið 1991: Gjóskufallið og gjóskulagið fráfyrsta degi gossins (the Hekla eruption of 1991 - the tephra fall) (in Icelandic with English summary), *Náttúrufræðingurinn*, *61*, 159–176.

Leadbetter, S., and M. C. Hort (2011), Volcanic ash hazard climatology for an eruption of Hekla Volcano, Iceland, *J. Volcanol. Geotherm. Res.*, *199*, 241–320.

Mastin, L. (2007), A user-friendly one-dimensional model for wet volcanic plumes, *Geochem. Geophys. Geosyst.*, *8*, Q03014, doi:10.1029/2006GC001455.

Morton, B. R., G. Taylor, and J. S. Turner (1956), Turbulent gravitational convection from maintained and instantaneous sources, *Proc. R. Soc. A*, *234*, 1–23, doi:10.1098/rspa.1956.0011.

Oddson, B. (2007), The Grímsvötn eruption in 2004: Dispersal and total mass of tephra and comparison with plume transport models, Master's thesis, Univ. of Iceland, Reykjavik.

Oman, L., A. Robock, G. Stenchikov, G. A. Schmidt, and R. Ruedy (2005), Climatic response to high-latitude volcanic eruptions, *J. Geophys. Res.*, *110*, D13103, doi:10.1029/2004JD005487.

Petersen, G. N. (2010), A short meteorological overview of the Eyjafjallajökull eruption 14 April–23 May 2010, *Weather*, *65*, 203–207, doi:10.1002/wea.634.

Prata, A. J. (2009), Satellite detection of hazardous volcanic clouds and the risk to global air traffic, *Nat. Hazards*, *51*, 303–304, doi:10.1007/s11069-008-9273-z.

Prata, A. J., and A. Tupper (2009), Aviation hazards from volcanoes: The state of the science, *Nat. Hazards*, *51*, 239–244, doi:10.1007/s11069-009-9415-y.

Robock, A. (2000), Volcanic eruptions and climate, *Rev. Geophys.*, *38*(2), 191–219.

Schumann, U., et al. (2011), Airborne observations of the Eyjafjalla volcano ash cloud over Europe during air space closure in April and May 2010, *Atmos. Chem. Phys.*, *11*, 2245–2279, doi:10.5194/acp-11-2245-2011.

Settle, M. (1978), Volcanic eruption clouds and the thermal power output of explosive eruptions, *J. Volcanol. Geotherm. Res.*, *3*, 309–324, doi:10.1016/0377-0273(78)90041-0.

Sigmundsson, F., and M. T. Gudmundsson (2004), Gos í Grímsvötnum 1.-6. nóvember 2004 (Grímsvötn eruption, November 1–6, 2004) (in Icelandic with English summary), *Jökull*, *54*, 139–142.

Skamrock, W. C., J. B. Klemp, J. Dudhia, D. O. Gill, D. M. Barker, W. Wang, and J. G. Powers (2005), A description of the advanced research WRF version 2, *NCAR Tech. Note 468+STR*, Natl. Cent. for Atmos. Res., Boulder, Colo.

Sparks, R. S. J. (1986), The dimensions and dynamics of volcanic eruption columns, *Bull. Volcanol.*, *48*, 3–15, doi:10.1007/BF01073509.

Sparks, R. S. J., and L. Wilson (1982), Explosive volcanic eruptions - V. Observations of plume dynamics during the 1979 Soufriere Eruption, St. Vincent, *Geophys. J. R. Astron. Soc.*, *69*(2), 551–570.

Stohl, A., M. Hittenberger, and G. Wotawa (1998), Validation of the lagrangian particle dispersion model flexpart against large scale tracer experiments, *Meteorol. Appl.*, *32*, 4245–4264.

Thorarinsson, S. (1970), *Hekla*, 59 pp., Almenna Bókafélagið, Reykjavík.

Thorarinsson, S., and G. R. Sigvaldason (1972), The Hekla eruption of 1970, *Bull. Volcanol.*, *36*, 269–288.

Tupper, A., J. S. Oswalt, and D. Rosenfeld (2005), Satellite and radar analysis of the volcanic-cumulonimbi at Mt Pinatubo, Philippines, 1991, *J. Geophys. Res.*, *110*, D09204, doi:10.1029/2004JD005499.

Tupper, A., C. Textor, M. Herzog, H.-F. Graf, and M. S. Richards (2009), Tall clouds from small eruptions: the sensitivity of eruption height and fine ash content to tropospheric instability, *Nat. Hazards*, *51*, 375–401, doi:10.1007/s11069-009-9433-9.

Vogfjörd, K. S., et al. (2005), Forecasting and monitoring a subglacial eruption in Iceland, *Eos Trans. AGU*, *86*(26), 245, doi:10.1029/2005EO260001.

Welander, P. (1955), Studies on the general development of motion in a two-dimensional, ideal fluid, *Tellus*, *7*, 141–156, doi:10.1111/j.2153-3490.1955.tb01147.x.

Wilson, L. (1976), Explosive volcanic eruptions - III. Plinian eruption columns, *Geophys. J. R. Astron. Soc.*, *45*, 543–556, doi:10.1111/j.1365-246X.1976.tb06909.x.

Wilson, L., R. S. J. Sparks, T. C. Huang, and N. D. Watkins (1978), The control of volcanic column heights by eruption energetics and dynamics, *J. Geophys. Res.*, *83*(B4), 1829–1836, doi:10.1029/JB083iB04p01829.

Wilson, L., R. S. J. Sparks, T. C. Huang, and N. D. Watkins (1987), Explosive volcanic eruptions - VI. Ejecta dispersal in plinian eruptions: The control of eruption conditions and atmospheric properties, *Geophys. J. R. Astron. Soc.*, *89*, 657–679, doi:10.1111/j.1365-246X.1987.tb05186.x.

Witham, C. S., M. C. Hort, R. Potts, R. Servranckx, P. Husson, and F. Bonnardot (2007), Comparison of VAAC atmospheric dispersion models using the 1 November 2004 Grimsvötn eruption, *Meteorol. Appl.*, *14*, 27–38.

Woods, A. W. (1988), The fluid dynamics and thermodynamics of eruption columns, *Bull. Volcanol.*, *50*, 169–193, doi:10.1007/BF01079681.

P. Arason, H. Bjornsson, and G. N. Petersen, Icelandic Meteorological Office, Bústaðavegur 9, IS-150 Reykjavík, Iceland. (gnp@vedur.is)